*Int. J. Morphol.,*
*43(3)*:1001-1010, 2025.

# Ferrostatin-1 Partially Suppressed the Anti-Fibrotic Actions of Thymoquinone in a Rat Model of Cholestasis-Induced Liver Injury

## La Ferrostatina-1 Suprimió Parcialmente las Acciones Antifibróticas de la Timoquinona en un Modelo de Rata con Lesión Hepática Inducida por Colestasis

**Hend Ashour[1]; Hind Zafrah[1]; Muataz Elsiddig Dafaalla Mohammed[1]; Laila Ahmed Rashed[2]; Abbas Mohamed Abbas[2]; Samaa Samir Kamar[3,4] & Asmaa Mohammed ShamsEldeen[5]**

**ASHOUR, H.; ZAFRAH, H.; MOHAMMED, M. E. D.; RASHED, L. A.; ABBAS, A. M.; KAMAR, S. S. & SHAMSELDEEN, A. M.** Ferrostatin-1 partially suppressed the anti-fibrotic actions of thymoquinone in a rat model of cholestasis-induced liver injury. *Int. J. Morphol., 43(3)*:1001-1010, 2025.

**SUMMARY:** Cholestasis is a leading cause of hepatic fibrosis. The herbal plant thymoquinone (TQ) has a well-known hepatoprotective effect against liver fibrosis. In this study, we investigated the role of ferroptosis in TQ-mediated antifibrotic action in a rat model of extrahepatic cholestasis developed secondary to bile duct ligation (BDL). Four groups (n=10) of adult male Wistar albino rats were included in the study; 1) control, 2) BDL model, 3) treated group with 50 mg.kg-1.day-1 TQ, and group 4) rats in this group were treated with TQ and the ferroptosis inhibitor, ferrostatin-1 (Fer-1) at a dose of 1 mg.kg-1.day-1. TQ treatment effectively attenuated the inflammation and fibrosis detected in the BDL group by modulating ($P<0.01$), NF-κB, TNF-α, interleukins; IL-6, 10, TGFβ-1, collagen type I, III. TQ improved liver function which was confirmed by histological H&E and Sirius red stain. TQ augmented ($p<0.001$) the heme oxygenase (HO-1) protein levels about 4 fold compared to the BDL group suggesting its role in hepatic protection. TQ stimulated the ferroptosis process and increased glutathione peroxidase (GPX4), Iron content, and the transferrin receptor (TfR-1). Fer-1 addition to TQ did not affect the anti-inflammatory actions of TQ. However, it significantly ($p<0.001$) attenuated its antifibrotic property. In conclusion, The antifibrotic effect of Thymoquinone was partially inhibited secondary to Fer-1. Thus, documenting the mediating role of ferroptosis in the TQ protection against hepatic fibrosis.

**KEY WORDS: Liver fibrosis; Cholestasis; Ferroptosis; Ferrostatin; Thymoquinone.**

## INTRODUCTION

Cholestasis is a major emerging cause of hepatic fibrosis. The bile accumulation distorts the hepatic architecture, increases the risk of cirrhosis and later on hepatocellular carcinoma (HCC). The main cellular constituents of liver tissue are hepatocytes (about 60 %). Meanwhile, the hepatic stellate cells (HSCs) contribute about 10-25 % of the liver cells. HSCs are located in the perisinusoidal area (Vekemans & Braet, 2005). Following cholestasis, HSCs are activated and transdifferentiated from quiescent cells into proliferative myofibroblasts contractile cells which can secrete collagen. Therefore, HSC activation serves as the primary mediator of hepatic fibrosis (Cai & Boyer, 2021).

Ferroptosis is a recently reported new mode of regulated cell death. Its essential characteristics are disturbed redox homeostasis, iron overload, and enhanced lipid peroxidation. Ferroptosis is closely related to developing and controlling various liver diseases, such as steatohepatitis, fibrosis, and HCC (Zhu *et al*., 2021). Cellular iron overload that accounts for iron-mediated oxidative stress (Yu *et al*., 2020), is mainly imported by the plasma membrane protein transferrin receptor (TfR-1)-mediated endocytosis and stored within ferritin or undergoes Fenton reaction and lipid peroxidation (Tang *et al*., 2023). Interestingly, the prominent higher affinity of receptor TfR-1 on activated HSCs indicates the importance of iron in HSCs regulation (Bridle *et al*.,

[1] Department of Physiology, Faculty of Medicine, King Khalid University, Abha, Saudi Arabia.
[2] Department of Biochemistry and Molecular Biology, Kasralainy Faculty of Medicine, Cairo University, Egypt.
[3] Department of Histology, Kasr Al-Ainy Faculty of Medicine, Cairo University, Egypt.
[4] Department of Histology, Armed Forces College of Medicine, Cairo, Egypt.
[5] Department of Physiology, Kasralainy Faculty of Medicine, Cairo University, Egypt.
FUNDING. This research was funded by the Research Deanship of King Khalid University, Abha, Saudi Arabia; Grant number No. RGP 1/31/45.

Received: 2024-12-12 Accepted: 2025-02-15

2003). However, it is unclear whether iron overload promotes HSCs activation and fibrosis formation, or it directs the cells to ferroptosis and hinders the fibrosis process. Several recent studies showed that Fer-1 inhibitor blocks the activity of some antifibrotic agents (Zhang *et al*., 2018; Yuan *et al*., 2022). Therefore, targeting ferroptosis could be a promising therapeutic approach for hepatic fibrosis.

Thymoquinone (TQ), the main constituent of Nigella sativa, has long been focused on treating liver diseases in recent years. TQ has a variety of beneficial hepatic antioxidant and anti-inflammatory activities (Farghaly *et al*., 2022). The induction of HO-1 by TQ has been reported in several tissues, including the liver (Licari *et al*., 2019). Heme oxygenase (HO) is a ubiquitous and essential enzyme for eukaryotic cells that converts heme into biliverdin, carbon monoxide, and iron. Upregulation of HO-1 revealed cytoprotective mechanisms against inflammation, ischemia, and hypoxia through maintaining antioxidant/oxidant homeostasis (Sasson *et al*., 2021). Moreover, during the early stages of fibrosis, HO-1 induction was able to regress portal inflammation and fibrosis (Barikbin *et al*., 2012). Besides the anti-apoptotic effect of HO-1 on hepatocytes (Sass *et al*., 2004). HO-1 promoted HSCs ferroptosis and ameliorated CCl4-mediated hepatic fibrosis (Sui *et al*., 2018). Therefore, HO-1 seems to possess a dual role in liver cell viability and proliferation, which may be the way for hepatocyte survival and HSC senesces performed by thymoquinone treatment.

This study aims to investigate the protective role of thymoquinone in alleviating BDL-induced liver fibrosis and to examine the possible role of ferroptosis using Fer-1.

## MATERIAL AND METHOD

**Animals and study groups**. Forty adult male Wister albino rats weighing 250-270 g were enrolled in the current study. The experimental protocol was approved by the institutional animal care and use committee of Cairo University (III/F/72/22). Following acclimatization, the rats were assigned into four groups (n=10): 1- Control group: rats were exposed to the same procedures of the BDL operation without ligation, 2- liver fibrosis induced by bile duct ligation (BDL)-induced cholestasis for three weeks, 3- group treated with thymoquinone 50 $mg.kg^{-1}$ once a day by gavage for the same duration (BDL-TQ) (Kong *et al*., 2015). In group 4 (BDL-TQ-Fer-1), the rats were treated with thymoquinone as in group 3 and the ferroptosis inhibitor, ferrostatin-1, at a dose of 1 mg/kg/day intraperitoneal (Yi *et al*., 2021). Thymoquinone and ferrostatin-1 were obtained from Sigma Chemical company, St Louis, MO, USA, and were dissolved in DMSO and saline.

**Induction of Extrahepatic model of cholestasis by BDL operation.** The rats were anesthetized with ketamine (150 µg/g) and xylazine (3 µg/g) (Mishra, 2003), and the anterior abdomen wall was shaved and disinfected with an alcohol solution. Following the procedures mentioned in (ShamsEldeen *et al*., 2021), a midline laparotomy incision of approximately 1-1.5 cm was performed. The common bile duct was identified and gently separated from the surrounding fascia. Double surgical sutures were placed, then, 300 mL of warm saline solution was administered intraperitoneally before the abdominal closure to prevent dehydration. All rat groups were kept for 3 weeks under close observation with or without treatment.

**Humane endpoint, samples collection and preparation.** Under pentobarbital (50 $mg.kg^{-1}$/i.p) general anesthesia, blood samples were drawn from the abdominal aorta to prepare serum. Then, animals were culled by cervical dislocations, and liver tissues were harvested, cleaned, rinsed with heparinized saline, and then weighed. Liver specimens were preserved in formaldehyde and prepared for histological analysis. The remaining liver tissues were minced into small pieces, homogenized in phosphate-buffered saline (PBS), and centrifuged for about 15 min at 1500×g. The formed supernatants were collected and stored at -80 °C.

**Biochemical analysis.** All steps followed the manufacturer's instructions.

**Liver function determination using serum levels of transaminases, bilirubin, and liver tissue iron content.** The serum liver enzymes were assessed using a colorimetric endpoint method, alanine aminotransferase (ALT; using BioMed-GPT, BioMed diagnostics, Egypt) and aspartate aminotransferase (AST; BioMed Diagnostic-GOT, BioMed diagnostics, Egypt). Total bilirubin levels were detected by bilirubin assay kit # ab235627 (Abcam, Kemet Medical, Giza, Egypt). The total iron content ($Fe^{2+}$ and $Fe^{3+}$) in the liver was measured using the iron assay kit #ab83366 provided by Abcam, Kemet Medical, Giza, Egypt.

**Western blot analysis for liver HO-1.** Total protein extraction was performed using a ReadyPrepTM kit (Bio-Rad Inc., Hercules, CA, catalog. No: 163–2086). Then, as described previously, protein samples of 20 µg were immunoblotted (Ashour *et al*., 2021). Membranes were maintained overnight at 4 °C with the primary antibody for HO-1 (# MA1-112; Invitrogen, Thermo Scientific, Waltham, MA). At room temperature, the blots were incubated for about one hour with the secondary antibody (# 11-4817-82, Invitrogen, Thermo Scientific, Waltham, MA). The protein plots were assessed, analyzed, and then normalized to the b-actin (# AM4302, Invitrogen, Thermo Scientific, Waltham, MA).

**Enzyme-linked immunosorbent assay (ELISA) for liver tissue inflammatory, fibrosis, and peroxidation markers.** Quantification determination was done based on sandwich ELISA technology. Nuclear factor-κB kits were obtained from CUBIO Innovation Center, Houston, USA (NF-κB: #CSB-E13148r). The following ELISA kits were attained from MyBioSource (Science and Technology Center, Giza, Egypt); tumor necrosis factor (TNF-α: # BMS622), interleukins; (IL-6: # MBS2021530), (IL-10: # MBS2020828), and glutathione peroxidase (GPX4: #MBS069787). Transforming growth factor Beta-1(TGFβ-1: ab119558), collagen type I ELISA Kits #ab285314, and the collagen type III #MBS762380 were retrieved from Abcam, Kemet Medical, Giza, Egypt.

**Quantitative real-time polymerase chain reaction (qPCR) for detection of relative gene expression of transferrin receptor (TfR-1. (**Total RNA was isolated. Complementary strands of cDNA were prepared by reverse transcription of total RNA. The amplification and analysis were carried out using an Applied Biosystem with software version 3.1 (StepOne™, Applied Biosystems, Lincoln Centre Drive, Foster City, CA). The data that was obtained was assessed and relatively normalized to the expression of housekeeping β-actin mRNA. The primer sequences for TfR-1 expression GenBank: M58040.2, Forward: 5'-GAGGAACCAGACCGCTACAT-3' Reverse: 5'-ATGTAGCGGTCTGGTTCCTC-3' and for the β-actin GenBank: KJ696744, Forward: 5'-AGCCATGTACGTAGCCATCCA-3' Reverse: 5'-TCTCCGGAGTCCATCACAATG-3'.

**Histological examination.** Specimens from liver tissue were fixed in 10 % formaldehyde solution and then processed as paraffin blocks. Unstained sections (4 μm thickness) were subjected to hematoxylin and eosin (H&E) and Sirius red staining. Liver injury was assessed using histological scoring for the H&E stained sections at magnification (×200) as follows: 0= normal appearance; 1=mild injury (up to 10 % of the liver tissue); 2=moderate injury (up to 50 % of the liver tissue); and 3=severe injury (up to 100 % of the liver tissue) (Heijnen *et al*., 2003).

**Statistical analysis.** The data were analyzed using the Statistical Package for the Social Sciences (SPSS, version 20), and expressed as mean ± SD. Comparison between groups was assessed by the Analysis of variance (ANOVA) test followed by Tukey's post-hoc test. The histology scoring for hepatic injury was analyzed by the non-parametrical Kruskal–Wallis and Mann–Whitney tests and was expressed as the median and interquartile range (50 %; 25 %-75 %). Statistical difference was significant if the p-value was < 0.05.

## RESULTS

**Liver weight/body weight ratio and liver functions.** The gross pictures in Figure 1 (A) demonstrate enlarged liver size in the BDL group, which was reduced in the treated group BDL-TQ. By adding Fer-1 to the treatment, liver size remained increased. The ratio between liver weights and body weights was significantly enhanced (P<0.001) in the BDL group compared to controls. By TQ treatment, the ratio significantly declined (P<0.001) compared to the BDL group. However, adding Fer-1 decreased ratio (P<0.05) compared to BDL and a maintained elevated ratio (P<0.001) compared to the BDL-TQ group (Fig. 1B). ALT, AST, and total bilirubin analysis levels deteriorated (P<0.001) in the BDL group, which was significantly (P<0.001) improved in the BDL-TQ group compared to the BDL model. Although adding

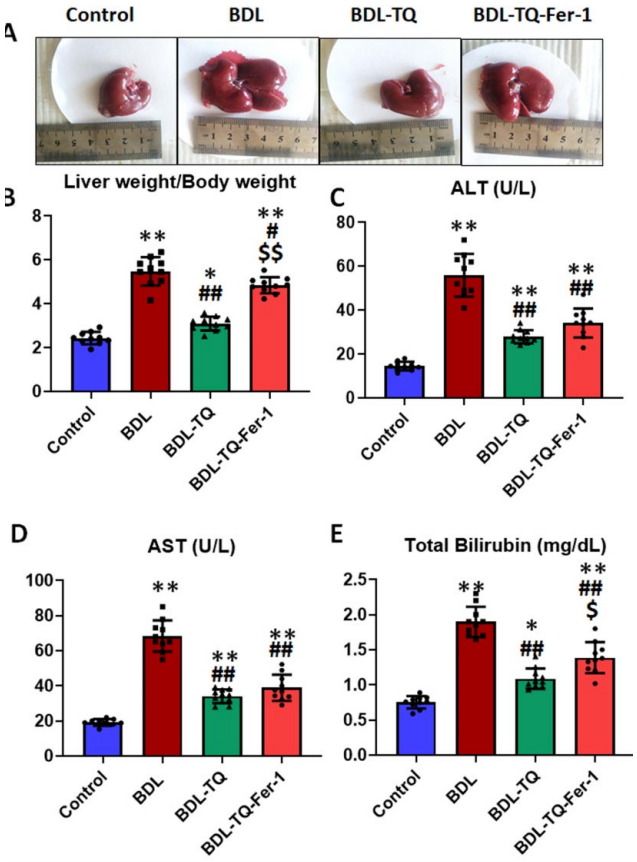


Fig. 1. A) Gross liver pictures obtained following 3 weeks of cholestasis from each experimental group. B) Calculation of the liver weight/Body weight ratio. The serum levels of C) ALT: alanine aminotransferase, D) AST: aspartate aminotransferases, and E) total bilirubin level (n=10). BDL: bile duct ligation, TQ: Thymoquinone, Fer-1: ferrostatin-1; a ferroptosis inhibitor, (n=10) *: significant to control when P<0.05. **: significant to control when P<0.001. #: significant to BDL when P<0.05. ##: significant to BDL when P<0.001. $: significant to BDL-TQ when P<0.05. $$: significant to BDL-TQ when P<0.001.

Fer-1 did not significantly affect ALT and AST compared to the BDL-TQ group, the results document a significantly increased liver weight and bilirubin level compared to the BDL-TQ group (Figs. 1C-E).

**Histological examination by H&E and the score of injury.** The BDL group showed severe liver damage with large necrotic areas, bile duct hyperplasia, and enhanced fibrosis around the portal areas. BDL-TQ group illustrated preservation in most of the liver parenchyma with a significant decrease (P<0.001) in liver damage scoring (1; 0.75-1.25) as compared to the BDL (3; 2-3). The BDL-TQ-Fer-1 group (1; 1-2) showed no statistical difference from the BDL-TQ group (Fig. 2).

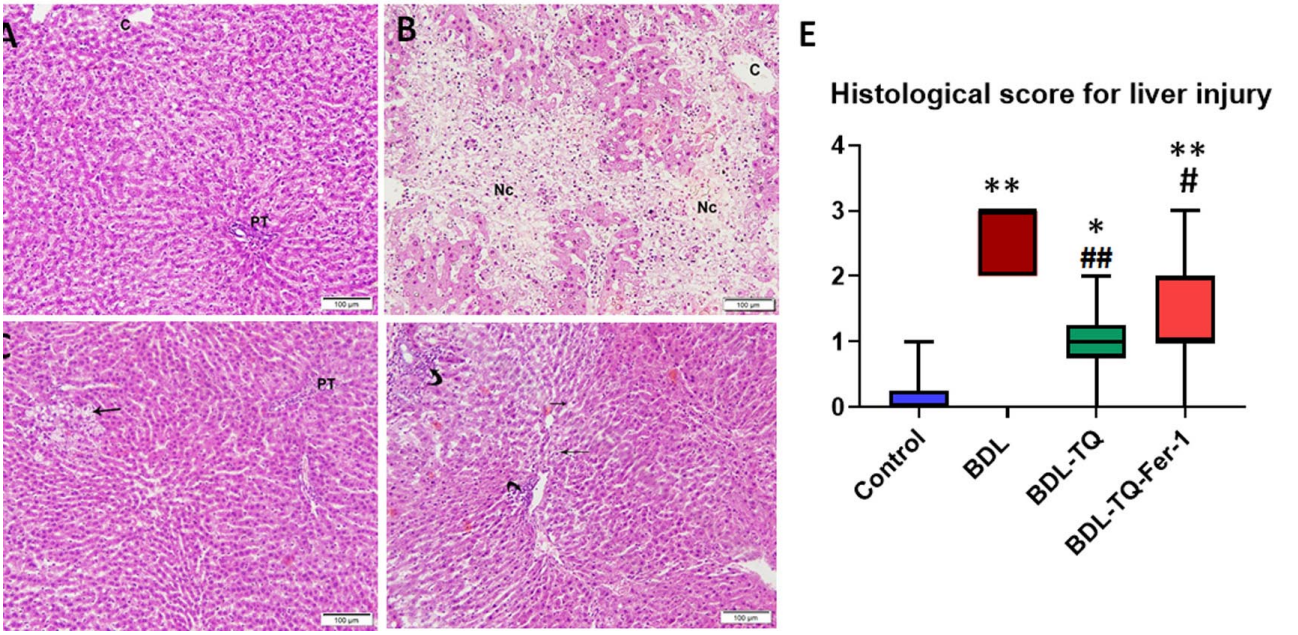


Fig. 2. Photomicrographs of H&E stained-liver sections (x100) shows: A) Control group: portal tract (PT), central vein (C) and cords of hepatocytes displaying vesicular nuclei and acidophilic cytoplasm. B) BDL-group: distorted liver parenchyma by multiple large necrotic areas (Nc) showing degenerated cells and inflammatory cells. C) BDL+TQ: preserved liver parenchyma with hepatocytes surrounding portal tract (PT). Small area of hepatocytes showing cytoplasmic vaculation (arrow) were noted. D) BDL-TQ+Fer-1: inflammatory cells infiltration (curved arrow) and diffuse cytoplasmic vacuolation of hepatocytes (arrow), (n=10). BDL: bile duct ligation, TQ: Thymoquinone, Fer-1: ferrostatin-1; a ferroptosis inhibitor. *: significant to control when P<0.05. **: significant to control when P<0.001. #: significant to BDL when P<0.05. ##: significant to BDL when P<0.001.

**Heme oxygenase-1 and glutathione peroxidase (GPX4).** The BDL group showed no significant P=0.55 change in HO-1protien expression, while GPX4 was significantly diminished (P<0.001). In the treated group BDL-TQ, augmented (P<0.001) HO-1 and GPX4 levels compared to both control and BDL groups. Interestingly, by adding Fer-1 to the treatment in group BDL-TQ-Fer-1 observed similar results of HO-1 (P=0.941) and GPX4 (P=0.1) to the data in the BDL-TQ group (Figs. 3A,B).

**The hepatic iron content and transferrin receptor expressions.** Levels of hepatic iron content and the TfR-1 were enhanced (P<0.001) in the BDL group compared to control. Additional expressions were documented (P<0.001) in the BDL-TQ group compared to BDL data. In the BDL-TQ-Fer-1 group, the results showed reduced (P= 0.026 and 0.001) for iron and TfR-1 expression, respectively, compared to the TQ-Fer-1 group, but still significantly elevated (P<0.05) compared to the BDL data (Figs. 3C,D).

**Inflammatory markers detection in the liver tissues**. Analysis of the inflammatory markers revealed prominently (P<0.001) elevated NFkB, TNF-α, IL-6, and reduced IL-10 levels in the BDL group compared to the control group. Treatment with TQ showed a noticeable decline (P<0.001) in the NFkB, TNF-a, IL-6, and elevation in the IL-10 tissue levels. In the BDL-TQ-Fer-1 group, the inhibition of the ferroptosis process did not affect the anti-inflammatory effect of TQ, and the data was almost similar to that in the BDL-TQ group (Fig. 4).

**Histological examination with Sirius red-stained liver sections and fibrosis markers detection in the liver tissues.** Sirius red-stained liver sections supported the

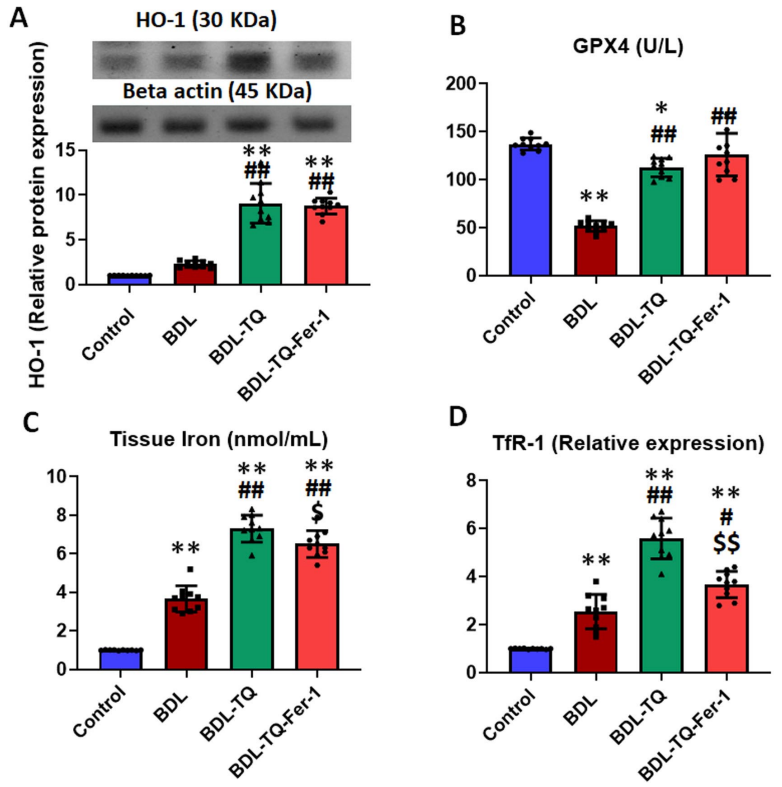


Fig. 3. A) Western blot determination of heme oxygenase-1 (HO-1) and western blot bands relative to b-actin, B) glutathione peroxidase (GPX4). PCR relative expressions of; C) total iron content, and D) transferrin receptor-1 (TfR-1), (n=10). BDL: bile duct ligation, TQ: Thymoquinone, Fer-1: ferrostatin-1; a ferroptosis inhibitor. *: significant to control when P<0.05. **: significant to control when P<0.001. #: significant to BDL when P<0.05. ##: significant to BDL when P<0.001. $: significant to BDL-TQ when P<0.05. $$: significant to BDL-TQ when P<0.001.

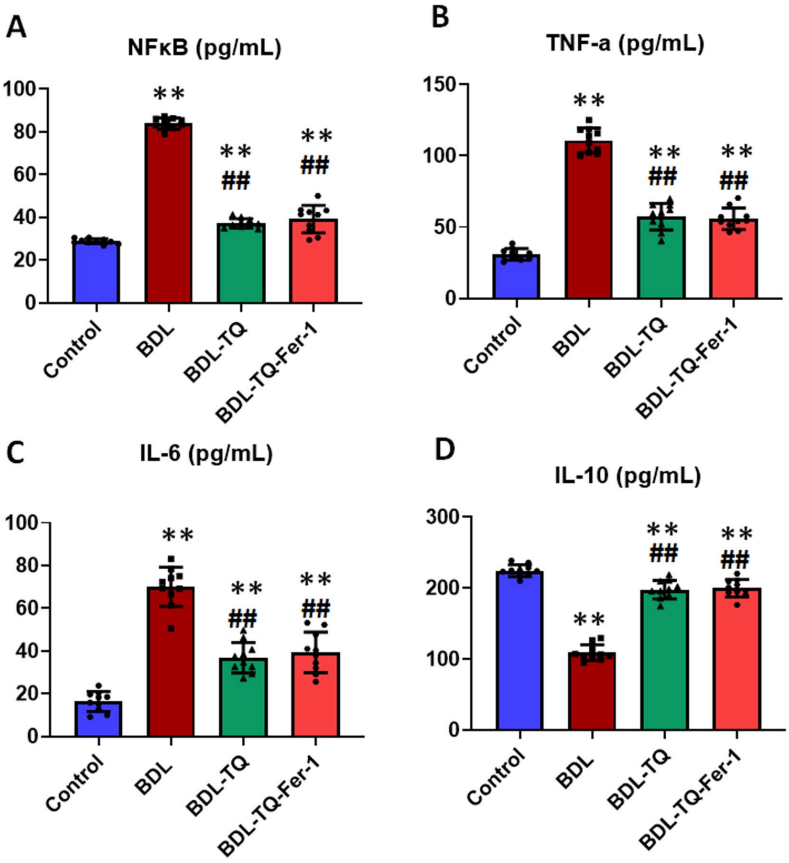


Fig. 4. Liver tissue analysis of the inflammatory markers A) nuclear factor kebab B (NFkB), B) Tumor necrosis factor alpha (TNF-a), C) interleukin-6 (IL-6, and D) interleukin-10 (IL-10), (n=10). BDL: bile duct ligation, TQ: Thymoquinone, Fer-1: ferrostatin-1; a ferroptosis inhibitor. **: significant to control when P<0.001. ##: significant to BDL when P<0.001.

biochemical analysis in Figure 5 (A-E). The BDL group showed extensive fibrosis around the portal areas with increased collagen area % (P<0.001). However, minimal fibrosis was detected following thymoquinone treatment (BDL-TQ), (P<0.001) compared to the BDL group. By blocking the ferroptosis process in the BDL-TQ-Fer-1 group, hepatic fibrosis was still preserved (P<0.001) compared with BDL-TQ.

The liver fibrosis was determined by elevated (P<0.001) tissue levels of TGFβ-1, collagen I, and collagen III in the BDL group compared with the control group. Treatment with TQ decreased (P<0.001) levels of all the profibrotic markers. While, the suppressed ferroptosis in the BDL-TQ-Fer-1 group maintained enhanced fibrosis similar (P= 0.12, 0.44, and 0.052, respectively) to that in the BDL group (Fig. 5).

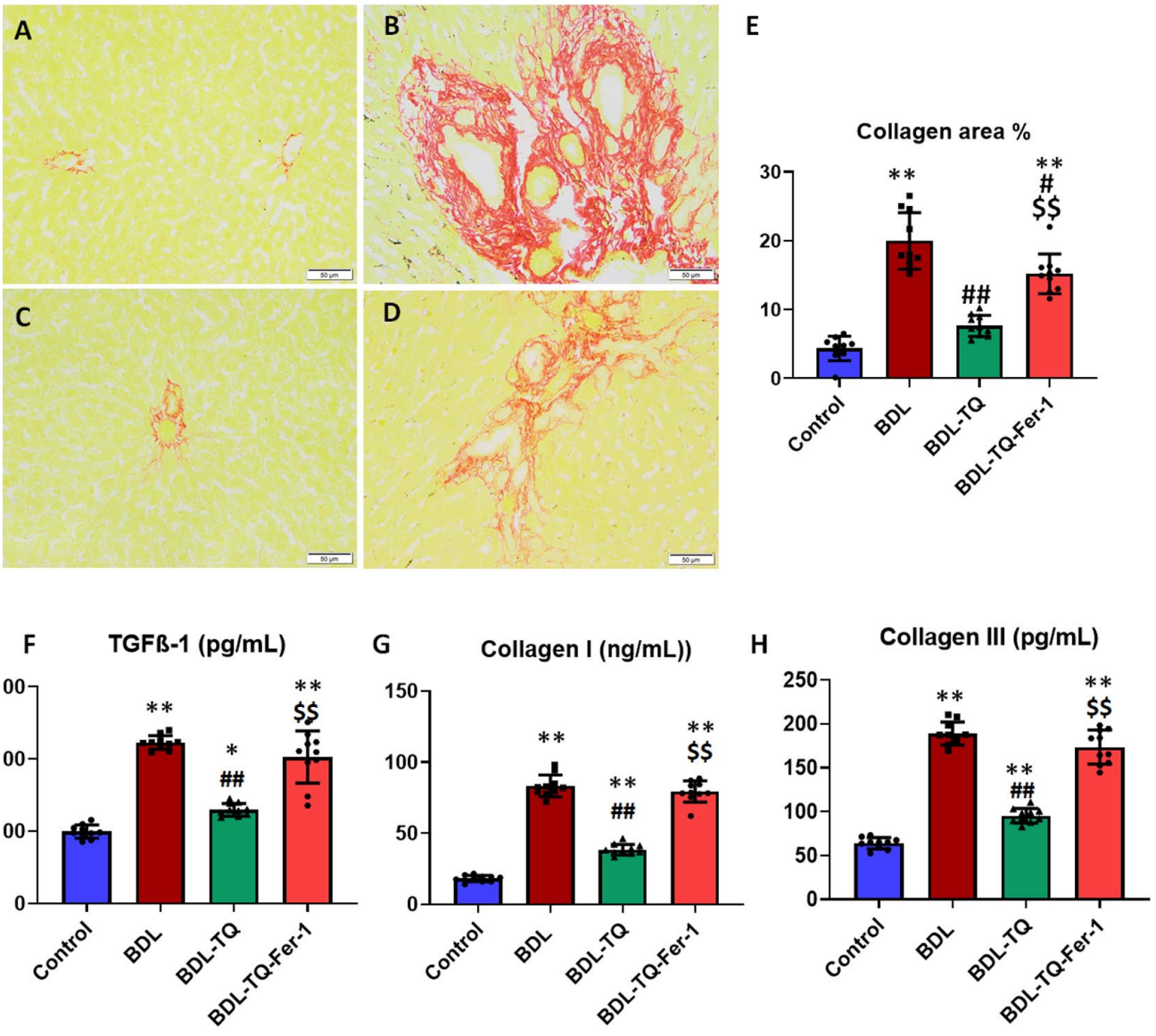


Fig. 5. Sirius red stained liver sections illustrates the collagen deposition in the studied groups A) Control group, B) BDL-induced fibrosis group, C) BDL-TQ, and D) BDL-TQ-Fer-1, and E) Collagen area percent was determined and analyzed. Liver tissue analysis of the fibrosis markers are represented in F) transforming growth factor beta-1 (TGFb-1), G) Collagen type I and H) collagen Type III. (n=10). BDL: bile duct ligation, TQ: Thymoquinone, Fer-1: ferrostatin-1; a ferroptosis inhibitor. *: significant to control when P<0.05. **: significant to control when P<0.001. #: significant to BDL when P<0.05. ##: significant to BDL when P<0.001. $$: significant to BDL-TQ when P<0.001.

## DISCUSSION

The experimental model of obstructive cholestasis obtained by surgical ligation of the common bile duct (CBD) is reliable for inducing liver fibrosis in rodents. It provokes time-dependent functional and structural changes in hepatic tissues (Van Campenhout *et al*., 2019). These changes range from hepatocyte injury with increased liver enzymes in the blood to a severe inflammatory reaction. The inflammatory reaction may occur within a few days, ending with advanced hepatic fibrosis that develops within 3-4 weeks after ligation (Tag *et al*., 2015). During cholestasis, the accumulation of bile acids damages the liver cells, recruits the inflammatory ones, and helps differentiation and activation of HSCs into myofibroblast with an enhanced ability to produce pro-fibrogenic mediators (Cai & Boyer, 2021), and excess reactive oxygen species (ROS), and TGF-β1 (ShamsEldeen *et al*., 2021). In the current study, we confirmed the existence of hepatic injury and collagen deposition biochemically and by histomorphometric examination. Notably, a significant increase in liver functions, and inflammatory and fibrosis markers in the liver tissues in the BDL group was confirmed compared to the control group.

Our results depicted the protective effect of TQ in a cholestasis rat model. TQ has been scientifically documented to possess hepatic antioxidative, anti-inflammatory, and anticancer properties demonstrated in reduced ALT, AST, and bilirubin levels (Ashour *et al*. 2023). TQ successfully reduced the levels of TNF-α and NF-κB in hepatic tissues. Consequently, it prevented the transcription of target genes, including different pro-inflammatory cytokines and chemokines, thus protecting the animals from hepatic inflammation and injury (Chen *et al*., 2020). It is worth saying that TQ exhibited anti-inflammatory properties by increasing IL-10 levels (Ashour *et al*., 2022). The impact of TQ on fibrotic liver injury was primarily ascribed to the inhibition of HSC activation induced by TGF-ß and the reduction in a-smooth muscle actin expression (Yang *et al*., 2016). Therefore, TQ effectively mitigated liver fibrosis as documented in several models such as cholestasis (Kong *et al*., 2015), CCL4 (Geng *et al*., 2021), and nonalcoholic steatohepatitis (Awad *et al*., 2016).

In recent decades, ferroptosis has started to attract scientists to explore its role in fibrosis (Zhou *et al*., 2022). Ferroptosis can exert a suppressive impact on liver fibrosis. This is likely achieved through the deactivation of HSCs and the induction of HSCs death (Wang *et al*., 2019). Under stressful disorders, iron metabolism is distorted and promotes the development of iron overload (Yu *et al*., 2020). Our results demonstrated enhanced expression levels of TfR-1 in the BDL group compared to the control group. The iron importer TfR-1 is a key protein responsible for regulating iron at both the systemic and cellular levels (Gao *et al*., 2022), which have previously been identified on activated HSC (Bridle *et al*., 2003).

The role of ferroptosis in the TQ protection against cholestasis was our target in this study. The induced HO-1 plays a crucial role in inflammatory processes and oxidative damage (Liu & Qian, 2015). In an *in vitro* study conducted by Xu *et al*. (2023), HO-1 can potentially trigger HSC apoptosis. This suggests that HO-1 could be a promising therapeutic target for preventing or reversing liver fibrosis. The overaccumulation of iron causes HO-1 production in hepatocytes and HSCs (Wu *et al*., 2021). The induction of ferroptosis in HSCs effectively mitigated liver injury and fibrosis through the promotion of iron enrichment and the upregulation of HO-1 levels (Tang *et al*., 2023).

HO-1 appears to have a dual impact on the viability and proliferation of liver cells. It disrupts chronic hepatic inflammation, which could potentially promote the survival of hepatocytes, whereas it can lead to senescence and death of HSCs (Canesin *et al*., 2022). Following our results, TQ effectively induces HO-1 in the liver tissues (Licari *et al*., 2019). Thus, the antifibrotic effect of TQ may be linked to the mediating role of HO-1 in inducing HSC ferroptosis and diminishing the expression of the profibrogenic mediators. In the same context, we demonstrated a significant increase in the expression levels of TfR-1 in the TQ-treated rats compared to the control and BDL groups.

Ferroptosis can be effectively inhibited by the synthetic antioxidant, Fer-1 (Jiang *et al*., 2022). The anti-ferroptotic effect of Fer-1 is similar to deferoxamine in a model of thioacetamide-induced acute liver injury by a mechanism involving iron chelation (Jiang *et al*., 2022). In this regard, we confirmed decreased iron content and expression of TfR-1 in the BDL-TQ-Fer-1 group compared to BDL-TQ group.

Inhibiting ferroptosis by using Fer-1 could block the anti-fibrosis potential of some agents, such as Erastin, and sorafenib (Zhang *et al*., 2018), and celastrol (Luo *et al*., 2022), and strongly reduce the artemether-induced antifibrosis effect (Wang *et al*., 2019). Therefore, the current findings showed that inhibition of ferroptosis secondary to Fer-1 intake was able to attenuate TQ-mediated fibrosis suppression.

## CONCLUSION

TQ alleviated chronic hepatic inflammation and down-regulated production of pro-inflammatory cytokines. In our results, TQ exerted antioxidant and antifibrotic effects

and mitigated the production of pro-fibrogenic mediators together with inducing ferroptosis. However, the antifibrotic effect of Thymoquinone was partially inhibited by the anti-ferroptotic action of Fer-1 (Fig. 6).

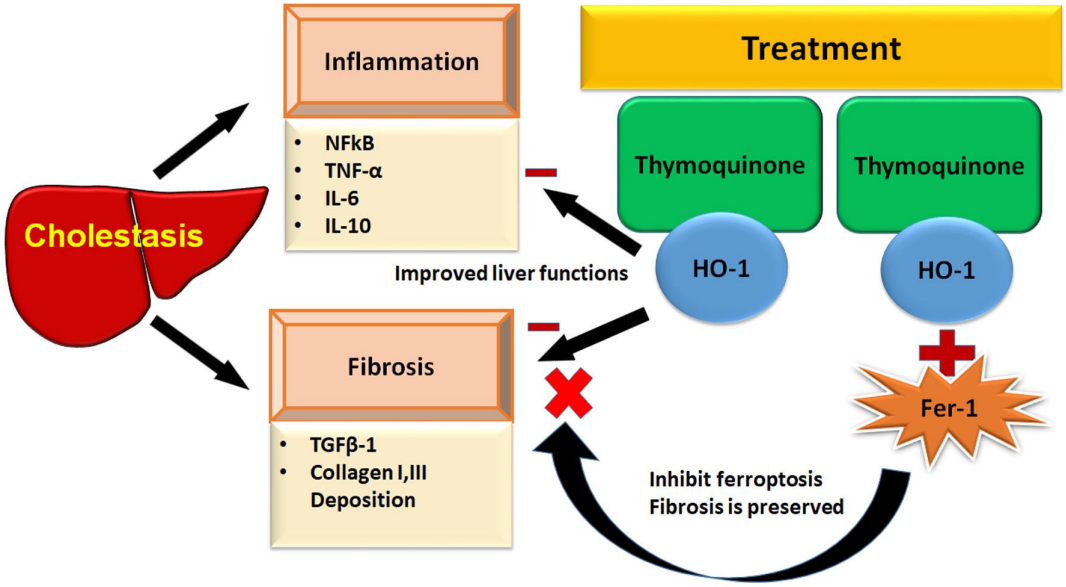


Fig. 6. A representative diagram demonstrates the protective effect of Thymoquinone in treating bile duct ligation-induced liver fibrosis. Thymoquinone induced the expression of Heme oxygenase-1 (HO-1) which may be the mediator for thymoquinone performance. Thymoquinone treatment resulted in anti-inflammatory anti-fibrosis property. By adding the ferroptosis inhibitor ferrostatin-1 (Fer-1), the results showed suppression of the antifibrotic effect of Thymoquinone. Therefore, it is concluded that thymoquinone antifibrotic effect could be mediated through ferroptosis of the hepatic fibrous producing cells. The inflammatory markers; nuclear factor kebab B (NFkB), tumor necrosis factor alpha (TNF-a), interleukin-6 (IL-6), and interleukin-10 (IL-10). The liver tissue fibrosis markers; transforming growth factor beta-1 (TGFβ-1), and collagen levels.

**Limitations and future recommendation:** in the current study, we focused on the in vivo role of ferroptosis linked to the therapeutic potential of Thymoquinone. The results documented a significant role of ferroptosis in ameliorating fibrosis which was suppressed by Fer-1. Thus, it is recommended that the work be extended to include an in vitro study on isolated hepatocytes and hepatic stellate cells to investigate the signaling pathways in each type of cell and to determine the specific role of HO-1.

**ACKNOWLEDGMENTS.** We are grateful to Dr Mariam Al-Ani from Face Studio Clinic, 273 Hagley Road, Birmingham, B16 9NB, UK for proofreading the manuscript.

**ASHOUR, H.; ZAFRAH, H.; MOHAMMED, M.E.D.; RASHED, L.A.; ABBAS, A.M.; KAMAR, S.S. y SHAMSELDEEN, A.M.** La ferrostatina-1 suprimió parcialmente las acciones antifibróticas de la timoquinona en un modelo de rata con lesión hepática inducida por colestasis. *Int. J. Morphol., 43*(3):1001-1010, 2025.

**RESUMEN:** La colestasis es una de las principales causas de fibrosis hepática. La planta herbácea timoquinona (TQ) posee un reconocido efecto hepatoprotector contra la fibrosis hepática. En este estudio, investigamos el papel de la ferroptosis en la acción antifibrótica mediada por TQ en un modelo de rata con colestasis extrahepática secundaria a la ligadura de la vía biliar (LVB). Cuatro grupos (n = 10) de ratas albinas Wistar macho adultas se incluyeron en el estudio: 1) control, 2) modelo BDL, 3) grupo tratado con 50 mg.kg-1.día-1 de TQ, y grupo 4) las ratas de este grupo fueron tratadas con TQ y el inhibidor de ferroptosis, ferrostatina-1 (Fer-1) a una dosis de 1 mg.kg-1.día-1. El tratamiento con TQ atenuó eficazmente la inflamación y la fibrosis detectadas en el grupo BDL modulando (P < 0,01), NF-kB, TNF-α, interleucinas; IL-6, 10, TGFβ-1, colágeno tipo I, III. TQ mejoró la función hepática que se confirmó mediante tinción histológica con H&E y rojo Sirio. TQ aumentó (p < 0,001) los niveles de proteína hemooxigenasa (HO-1) aproximadamente 4 veces en comparación con el grupo BDL, lo que sugiere su papel en la protección hepática. La TQ estimuló el proceso de ferroptosis y aumentó la glutatión peroxidasa (GPX4), el contenido de hierro y el receptor de transferrina (TfR-1). La adición de Fer-1 a la TQ no afectó sus acciones antiinflamatorias. Sin embargo, atenuó significativamente (p < 0,001) su propiedad antifibrótica. En conclusión, el efecto antifibrótico de la timoquinona se inhibió parcialmente como consecuencia de Fer-1. Por lo tanto, se documenta el papel mediador de la ferroptosis en la protección de la TQ contra la fibrosis hepática.

**PALABRAS CLAVE: Fibrosis hepática; Colestasis; Ferroptosis; Ferrostatina; Timoquinona.**

## REFERENCES

Ashour, H.; Farghaly, M. E.; Khowailed, A. A.; Aboulhoda, B. E.; Rashed, L. A.; Elsebaie, M. M. & Gaber, S. S. Modulation of miR-192/NF-kB/TGF-b/E-cadherin by thymoquinone protects against diethylnitrosamine/carbon tetrachloride hepatotoxicity. *Physiol. Int., 109(2)*, 2022.

Ashour, H.; Rashed, L.; Elkordy, M. A. & Abdelwahed, O. M. Remote liver injury following acute renal ischaemia–reperfusion: involvement of circulating exosomal miR-687 and regulation by thymoquinone. *Exp. Physiol., 106(12)*:2262-75, 2021.

Ashour, H.; Rashed, L. A.; Hassanein, R. T. M.; Aboulhoda, B. E.; Ebrahim, H. A.; Elsayed, M. H.; Elkordy, M. A. & Abdelwahed, O. M. Thymoquinone and quercetin protect against hepatic steatosis in association with SIRT1/AMPK stimulation and regulation of autophagy, perilipin-2, and cytosolic lipases. *Arch. Physiol. Biochem., 129(2)*:268-81, 2023.

Awad, A. S. M.; Abd Al Haleem, E. N.; El-Bakly, W. M. & Sherief, M. A. Thymoquinone alleviates nonalcoholic fatty liver disease in rats via suppression of oxidative stress, inflammation, apoptosis. *Naunyn Schmiedebergs Arch. Pharmacol., 389(4)*:381-91, 2016.

Barikbin, R.; Neureiter, D.; Wirth, J.; Erhardt, A.; Schwinge, D.; Kluwe, J.; Schramm, C.; Tiegs, G. & Sass, G. Induction of heme oxygenase 1 prevents progression of liver fibrosis in Mdr2 knockout mice. *Hepatology, 55(2)*:553-62, 2012.

Bridle, K. R.; Crawford, D. H. G. & Ramm, G. A. Identification and characterization of the hepatic stellate cell transferrin receptor. *Am. J. Pathol., 162(6)*:1661-7, 2003.

Cai, S. Y. & Boyer, J. L. The role of bile acids in cholestatic liver injury. *Ann. Transl. Med., 9(9)*:737, 2021.

Canesin, G.; Feldbrügge, L.; Wei, G.; Janovicova, L.; Janikova, M.; Csizmadia, E.; Ariffin, J.; Hedblom, A.; Herbert, Z. T.; Robson, S. C.; *et al*. Heme oxygenase-1 mitigates liver injury and fibrosis via modulation of LNX1/Notch1 pathway in myeloid cells. *iScience, 25*:104983, 2022.

Chen, W.; Li, Y.; Hsu, C. T.; Niu, C. S.; Pen, W. H.; Cheng, K. C. & Niu, H. S. Connective tissue growth factor in hepatocytes is elevated by carbon tetrachloride via STAT3 activation. *Mol. Med. Rep., 21(2)*:1390-8, 2020.

Farghaly, M. E.; Khowailed, A. A.; Aboulhoda, B. E.; Rashed, L. A.; Gaber, S. S. & Ashour, H. Thymoquinone potentiated the anticancer effect of cisplatin on hepatic tumorigenesis by modulating tissue oxidative stress and endoplasmic GRP78/CHOP signaling. *Nutr. Cancer, 74(2)*:278-87, 2022.

Gao, H.; Jin, Z.; Bandyopadhyay, G.; Wang, G.; Zhang, D.; Rocha, K. C. E.; Liu, X.; Zhao, H.; Kisseleva, T.; Brenner, D. A.; *et al*. Aberrant iron distribution via hepatocyte-stellate cell axis drives liver lipogenesis and fibrosis. *Cell Metab., 34(7)*:1201-1213.e5, 2022.

Geng, W.; Li, C.; Zhan, Y.; Zhang, R. & Zheng, J. Thymoquinone alleviates liver fibrosis via miR-30a-mediated epithelial-mesenchymal transition. *J. Cell. Physiol., 236(5)*:3629-40, 2021.

Heijnen, B. H.; Straatsburg, I. H.; Gouma, D. J. & van Gulik, T. M. Decrease in core liver temperature with 10°C by in situ hypothermic perfusion under total hepatic vascular exclusion reduces liver ischemia and reperfusion injury during partial hepatectomy in pigs. *Surgery, 134(6)*:806-17, 2003.

Jiang, H.; Zhang, X.; Yang, W.; Li, M.; Wang, G. & Luo, Q. Ferrostatin-1 ameliorates liver dysfunction via reducing iron in thioacetamide-induced acute liver injury in mice. *Front. Pharmacol., 13*:1-11, 2022.

Kong, L.Y.; Li, G.P.; Yang, P. & Xi, Z. Protective effect of thymoquinone on cholestatic rats with liver injury. *Genet. Mol. Res., 14(4)*:12247-53, 2015.

Licari, M.; Raffaele, M.; Rosman, Z. F.; Schragenheim, J.; Bellner, L. & Vanella, L. Beneficial effects of thymoquinone on metabolic function and fatty liver in a murine model of obesity. *J. Food Nutr. Sci., 9*:751, 2019.

Liu, B. & Qian, J. M. Cytoprotective role of heme oxygenase-1 in liver ischemia reperfusion injury. *Int. J. Clin. Exp. Med., 8(11)*:19867-73, 2015.

Luo, P.; Liu, D.; Zhang, Q.; Yang, F.; Wong, Y. K.; Xia, F.; Zhang, J.; Chen, J.; Tian, Y.; Yang, C.; *et al*. Celastrol induces ferroptosis in activated HSCs to ameliorate hepatic fibrosis via targeting peroxiredoxins and HO-1. *Acta Pharm. Sin. B, 12(5)*:2300-14, 2022.

Mishra, J. Identification of neutrophil gelatinase-associated lipocalin as a novel early urinary biomarker for ischemic renal injury. *J. Am. Soc. Nephrol., 14(10)*:2534-43, 2003.

Sass, G.; Seyfried, S.; Parreira Soares, M.; Yamashita, K.; Kaczmarek, E.; Neuhuber, W.L. & Tiegs, G. Cooperative effect of biliverdin and carbon monoxide on survival of mice in immune-mediated liver injury. *Hepatology, 40(5)*:1128-35, 2004.

Sasson, A.; Kristoferson, E.; Batista, R.; McClung, J. A.; Abraham, N. G. & Peterson, S. J. The pivotal role of heme oxygenase-1 in reversing the pathophysiology and systemic complications of NAFLD. *Arch. Biochem. Biophys., 697*:108679, 2021.

ShamsEldeen, A. M.; Al-Ani, B.; Ebrahim, H. A.; Rashed, L.; Badr, A. M.; Attia, A.; Farag, A. M.; Kamar, S. S.; Haidara, M. A.; Al Humayed, S.; *et al*. Resveratrol suppresses cholestasis-induced liver injury and fibrosis in rats associated with the inhibition of TGFb1–Smad3–miR21 axis and profibrogenic and hepatic injury biomarkers. *Clin. Exp. Pharmacol. Physiol., 48(10)*:1402-11, 2021.

Sui, M.; Jiang, X.; Chen, J.; Yang, H. & Zhu, Y. Magnesium isoglycyrrhizinate ameliorates liver fibrosis and hepatic stellate cell activation by regulating ferroptosis signaling pathway. *Biomed. Pharmacother., 106*:125-33, 2018.

Tag, C.; Weiskirchen, S.; Hittatiya, K.; Tacke, F.; Tolba, R. & Weiskirchen, R. Induction of experimental obstructive cholestasis in mice. *Lab. Anim., 49(1)*:70-80, 2015.

Tang, R.; Luo, J.; Zhu, X.; Miao, P. & Tang, H. Recent progress in the effect of ferroptosis of HSCs on the development of liver fibrosis. *Front. Mol. Biosci., 10*:1-12, 2023.

Van Campenhout, S.; Van Vlierberghe, H. & Devisscher, L. Common bile duct ligation as model for secondary biliary cirrhosis. *Methods Mol. Biol., 1981*:237-47, 2019.

Vekemans, K. & Braet, F. Structural and functional aspects of the liver and liver sinusoidal cells in relation to colon carcinoma metastasis. *World J. Gastroenterol., 11(33)*:5095-102, 2005.

Wang, L.; Zhang, Z.; Li, M.; Wang, F.; Jia, Y.; Zhang, F.; Shao, J.; Chen, A. & Zheng, S. P53-dependent induction of ferroptosis is required for artemether to alleviate carbon tetrachloride-induced liver fibrosis and hepatic stellate cell activation. *IUBMB Life, 71(1)*:45-56, 2019.

Wu, A.; Feng, B.; Yu, J.; Yan, L.; Che, L.; Zhuo, Y.; Luo, Y.; Yu, B.; Wu, D. & Chen, D. Fibroblast growth factor 21 attenuates iron overload-induced liver injury and fibrosis by inhibiting ferroptosis. *Redox Biol., 46*:102131, 2021.

Xu, Y.; Tong, Y.; Lei, Z.; Zhu, J. & Wan, L. Abietic acid induces ferroptosis via the activation of the HO-1 pathway in bladder cancer cells. *Biomed. Pharmacother., 158*:114154, 2023.

Yang, Y.; Bai, T.; Yao, Y. L.; Zhang, D.Q.; Wu, Y. L.; Lian, L. H. & Nan, J. X. Upregulation of SIRT1-AMPK by thymoquinone in hepatic stellate cells ameliorates liver injury. *Toxicol. Lett., 262*:80-91, 2016.

Yi, J.; Wu, S.; Tan, S.; Qin, Y.; Wang, X.; Jiang, J.; Liu, H. & Wu, B. Berberine alleviates liver fibrosis through inducing ferrous redox to activate ROS-mediated hepatic stellate cells ferroptosis. *Cell Death Discov., 7*:374, 2021.

Yu, Y.; Jiang, L.; Wang, H.; Shen, Z.; Cheng, Q.; Zhang, P.; Wang, J.; Wu, Q.; Fang, X.; Duan, L.; *et al*. Hepatic transferrin plays a role in systemic iron homeostasis and liver ferroptosis. *Blood, 136(6)*:726-39, 2020.

Yuan, S.; Wei, C.; Liu, G.; Zhang, L.; Li, J.; Li, L.; Cai, S. & Fang, L. Sorafenib attenuates liver fibrosis by triggering hepatic stellate cell ferroptosis via HIF-1a/SLC7A11 pathway. *Cell Prolif., 55(1)*:1-15, 2022.

Zhang, Z.; Yao, Z.; Wang, L.; Ding, H.; Shao, J.; Chen, A.; Zhang, F. & Zheng, S. Activation of ferritinophagy is required for the RNA-binding protein ELAVL1/HuR to regulate ferroptosis in hepatic stellate cells. *Autophagy, 14(12)*:2083-103, 2018.

Zhou, J.; Tan, Y.; Wang, R. & Li, X. Role of ferroptosis in fibrotic diseases. *J. Inflamm. Res., 15*:3689-708, 2022.

Zhu, Y.; Zhang, C.; Huang, M.; Lin, J.; Fan, X. & Ni, T. TRIM26 induces ferroptosis to inhibit hepatic stellate cell activation and mitigate liver fibrosis through mediating SLC7A11 ubiquitination. *Front. Cell Dev. Biol., 9*:644901, 2021.

Correspondening author:
Dr.Hend Ashour, Associate Professor
Physiology Department
Faculty of Medicine
King Khalid University
Abha
SAUDI ARABIA

ORCID: 0000-0002-5423-7228

E-mail: hiahmad@kku.edu.sa
hend.a.hassan@kasralainy.edu.eg